Organic Electronics 22 (2015) 62–68

Contents lists available at ScienceDirect

Organic Electronics

journal homepage: www.elsevier.com/locate/orgel

Charge carrier mobility of the organic photovoltaic materials PTB7 and $PC_{71}BM$ and its influence on device performance

Bernd Ebenhoch [a], Stuart A.J. Thomson [a], Kristijonas Genevičius [b], Gytis Juška [b], Ifor D.W. Samuel [a,*]

[a] Organic Semiconductor Centre, SUPA, School of Physics and Astronomy, University of St Andrews, St Andrews KY16 9SS, UK
[b] Department of Solid State Electronics, Vilnius University, Saulėtekio 9 III k., 10222 Vilnius, Lithuania

ARTICLE INFO

Article history:
Received 21 December 2014
Received in revised form 9 March 2015
Accepted 9 March 2015
Available online 11 March 2015

Keywords:
Time of flight
Temperature
Efficiency
Bimolecular recombination
Trap-assisted recombination

ABSTRACT

The mobility is an important parameter for organic solar cell materials as it influences the charge extraction and recombination dynamics. In this study, the time of flight technique is used to investigate the charge mobility of the important organic photovoltaic materials $PC_{71}BM$, PTB7 and their blend. The electron mobility of $PC_{71}BM$ is in the region of 1×10^{-3} cm^2/Vs for the neat fullerene film, and has a positive electric field dependence. At room temperature the hole mobility of PTB7 is 1×10^{-3} cm^2/Vs for the neat film and 2×10^{-4} cm^2/Vs for their blend. The hole mobility of the blend reduces by a factor of a thousand when the sample is cooled from room temperature to 77 K. This finding is compared with the device performance of efficient PTB7:$PC_{71}BM$ solar cells for varying temperature. At 77 K the solar cell efficiency halved, due to losses in fill factor and short circuit current. Bimolecular and trap-assisted recombination increase at low mobility (low temperature) conditions, whereas at high mobility conditions the open circuit voltage reduces. The power conversion efficiency as a function of temperature has a maximum between 260 K and 295 K, revealing an optimized mobility at room temperature.

1. Introduction

The polymeric donor material PTB7 (poly[[4,8-bis[(2-ethylhexyl)oxy]benzo[1,2-b:4,5-b′]dithiophene-2,6-diyl][3-fluoro-2-(2-ethylhexy)carbonyl]thieno[3,4-b]thiophenediyl]]) has attracted great interest in recent years due to its high performance in bulk heterojunction solar cells. Devices of PTB7 blended with $PC_{71}BM$ ([6,6]phenyl C71 butyric acid methyl ester) exhibit a high fill factor (FF) of up to 72% and external quantum efficiency (EQE) of 80% [1]. Both of these parameters are strongly influenced by the charge transport properties of the active layer. Accordingly this paper has two aims. The first is to report mobility measurements of these important and widely used solar cell materials. The second is to explore the influence of the mobility on device operation and charge recombination.

The main steps of operation in an organic solar cell are: light absorption, charge separation and charge transport to the electrodes. During charge transport of electrons in the acceptor phase and holes in the donor phase two types of recombination can occur which reduce the power conversion efficiency. Bimolecular recombination happens after an encounter between an electron and a hole in the material. This process is generally described by Langevin theory where the recombination rate R_B depends on the mobility and density of electrons and holes [2,3],

$$R_B = \frac{e}{\epsilon}(\mu_e + \mu_h)(np - n_i^2) \quad (1)$$

where ϵ is the dielectric constant ($\epsilon_0\epsilon_r$), e the elemental charge, μ_e and μ_h are the electron and hole mobility, n the electron density, p the hole density and n_i the density of intrinsic charge carriers. Since electrons and holes are created in pairs, R_B depends quadratically on the density of electrons stored in the device, n^2, which is generally much larger than the density of intrinsic charge carriers. Monomolecular recombination occurs when one charge carrier encounters an occupied trap state of immobile charge with the opposite sign. It is often described by a Shockley–Read–Hall (SRH) mechanism and depends on the density of trap states and is proportional to the density of mobile charge carriers, n [4,5]. The SRH recombination is given by the density of electron and hole trap states (n_{traps}, p_{traps}) and the lifetime of the trap state (τ_e, τ_h) and the rate constant is given by [6]

$$R_{SRH} = \frac{np - n_i^2}{\tau_e(n + n_{traps}) + \tau_h(p + p_{traps})} \quad (2)$$

* Corresponding author.
E-mail address: idws@st-andrews.ac.uk (I.D.W. Samuel).

http://dx.doi.org/10.1016/j.orgel.2015.03.013
1566-1199/

The mobility in disordered organic semiconductors is also influenced by trap states and the temperature, it decreases with decreasing temperature and increasing trap density [7].

To achieve a high external quantum efficiency of the solar cell, charges must be extracted faster than they recombine. The maximum extraction time is the device thickness divided by the drift velocity i.e. $d/\mu E$ where μ is the lowest mobility of electrons or holes, which should be similar, and E is the electric field.

$$\frac{d}{\mu E} < \frac{n}{R_B + R_{SRH}} \tag{3}$$

The above formalism shows the strong influence of the charge carrier mobility on the operation of photovoltaic devices. It is a crucial parameter for optimized device efficiencies and the time of flight (TOF) technique is the most accurate way to determine it. This paper reports the charge mobility for the important materials $PC_{71}BM$, PTB7 and their blend, measured by TOF with its electric field and temperature dependence. Although the influence of mobility on device operation has been explored theoretically [8–11], an experimental relation to the solar cell performance has not been deeply studied. Only recently a direct relation of mobility to device performance has been drawn in small molecule based solar cells for a variety of donor and acceptor blends and an increase of fill factor with increasing hole mobility was observed [12]. To further optimize devices it is important to know what role the mobility of the materials plays. For that, device characteristics were studied at low temperature (low mobility) and high temperature (high mobility) conditions and the associated recombination processes identified.

2. Materials and methods

PTB7 was purchased from 1-Material and $PC_{71}BM$ from Solenne. Neat films of $PC_{71}BM$ for TOF measurements were prepared from a solution of 49 mg/ml of $PC_{71}BM$ in tetrachloroethane. Films of neat PTB7 and blends of PTB7:$PC_{71}BM$ (1:1.5) were prepared from solutions of in total 40 mg/ml in 1,2-dichlorobenzene. For the blend 3 vol% diiodooctane was added to the solution. Glass substrates with a 4 mm stripe of ITO were cleaned with acetone, propan-2-ol and plasma ashing. For samples of $PC_{71}BM$, MoO_3 of about 8 nm thickness was thermally evaporated onto the ITO substrates, whereas for PTB7 and PTB7:$PC_{71}BM$ samples, PEDOT:PSS was spin coated instead and dried at 120 °C for 10 min. The active layer was then solution cast and dried overnight in a nitrogen glove box. The cathode of 15 nm calcium and 15 nm aluminum was thermally evaporated to create a semi-transparent contact. Three pixels with an area of 8 mm^2 were defined by the overlap of the anode and cathode. The film thickness was determined individually for each pixel by a surface profilometer after electrical characterization of the device.

Solar cells were fabricated in a similar way on PEDOT:PSS, using solutions of PTB7:$PC_{71}BM$ of 25 mg/ml concentration, spin coated at 1000 rpm to give films of 80 nm thickness. The aluminum thickness was 100–150 nm. Solar cells were encapsulated with a UV-curing epoxy and a glass slide.

TOF measurements were performed in a vacuum cryostat at less than 10^{-4} mbar pressure. The sample was excited by a tuneable nitrogen pumped dye laser using a wavelength of 640 nm for PTB7 or 337 nm for $PC_{71}BM$ and PTB7:$PC_{71}BM$ with a pulse-duration of 500 ps. The film thickness of the solution cast samples was much higher than the absorption depth, calculated from the absorption coefficient. Thus the condition that charges are generated in a thin sheet compared to the total layer thickness was clearly fulfilled. The laser power was attenuated so that the amount of extracted charge was small enough to avoid space charge effects but large enough to provide good signal to noise. For electron mobility measurements, the sample was excited from the ITO electrode and for hole mobility measurements through the calcium/aluminum electrode. In both cases positive bias was applied to the calcium/aluminum electrode, operating the device in reverse direction, to avoid charge injection. The photocurrent was measured with a digital storage oscilloscope. The temperature was regulated by the evaporation rate of liquid nitrogen and a heat source.

Solar cells were first measured under a class A, Sciencetech solar simulator and the intensity calibrated with an ORIEL reference cell with KG5 filter. The spectral mismatch factor was close to unity (0.995) for PTB7:$PC_{71}BM$ and not corrected for. An aperture of the same size as the pixel was used to avoid contribution from stray light outside the device area. The solar cell was then transferred into the cryostat and illuminated in a range of intensities from a collimated white-light LED. We took one sun illumination to be the LED intensity which gave the same current as measured under the simulator. The relative intensity of the LED was calibrated for linearity using a photodiode.

To obtain the EQE spectrum, the short circuit current of the solar cells was measured under monochromatic illumination and compared with a calibrated photodiode. Due to reflections on the cryostat window and the beam being larger than the device size an absolute value of EQE was not determined. Absorption of a PTB7:$PC_{71}BM$ film, spin coated onto a quartz substrate, was measured with the cryostat placed in the beam path of a Cary 300 spectrometer.

3. Results and discussion

3.1. Hole mobility of PTB7

The time of flight measurement technique is a widely used method for determining mobility and has several advantages over other methods. It measures the mobility perpendicular to the substrate, at low charge density, has simple data analysis protocols and has the advantage that electron and hole mobility can be distinguished in the same device configuration, and their dependence on the applied electric field determined. In neat PTB7, photocurrents with a pronounced kink were observed, which is in contrast to a recent publication by Philippa et al. who found very dispersive and featureless TOF transients [13]. An example of a photocurrent transient is shown in Fig. 1(a). The transit time was obtained on logarithmic plots by the intersection of a linear fit to the plateau and tail of the curve [14].

The hole mobility of PTB7 is approximately 1×10^{-3} cm^2/Vs at an applied electric field of 1.1×10^5 V/cm ($E^{0.5} = 335$ $(V/cm)^{0.5}$) and a film thickness of 8.3 μm. The effect of electric field on the mobility was measured and the results are shown as a Poole–Frenkel plot [15] in Fig. 1(b) and reveal only very weak field dependence. Our value of the hole mobility in PTB7 is slightly higher compared to results found by space charge limited current (SCLC) measurements, which were reported in the range $2–5.8 \times 10^{-4}$ cm^2/Vs [16–19]. The TOF mobility of PTB7 is almost one order of magnitude higher than that of P3HT for which reported values are about 2×10^{-4} cm^2/Vs [20].

3.2. Electron mobility of $PC_{71}BM$

Next we performed studies of the electron mobility of $PC_{71}BM$ by TOF. Mobility measurements of fullerenes by TOF so far were mainly done indirectly, either in blends with other conjugated polymers or an insulating matrix, because of the rather poor film quality of neat fullerene films [21]. The blend morphology and

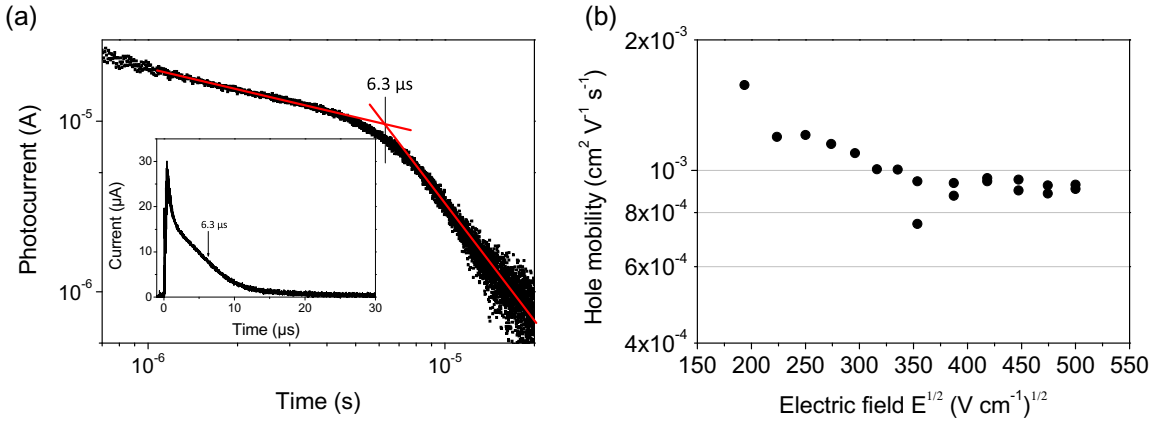

Fig. 1. (a) PTB7 photocurrent transient of conventional TOF at applied bias of 100 V, $E = 1.2 \times 10^5$ V/cm, on log–log scale and linear scale (inset). The sample is 8.3 µm thick. The carrier transit time is obtained from the characteristic kink in the log–log plot. (b) The hole mobility vs. electric field.

the fact that charges drift only in a part of the sample, can influence the mobility. For a fair comparison, mobility measurements of neat films are preferable. The solution cast films of $PC_{71}BM$ from tetrachloroethane with a finely tuned concentration of 39 mg/ml had a remarkably low surface roughness of 0.77 nm (root mean square) over the area of 20 × 20 µm and the film thickness of 2.8 µm of a typical pixel (2 mm × 4 mm) had a standard deviation of 3%. Besides the difficulty to fabricate thick fullerene layers, their deep lying HOMO level is another challenge. For the TOF technique charge carriers must be effectively extracted at the electrodes to avoid charge building up in the active layer, which would distort the electric field and impact the transit time. Molybdenum oxide (MoO_3) has a high work function of 6.8 eV [22], deeper than the HOMO level of $PC_{71}BM$, thus for holes the formation of an Ohmic contact, which provides efficient hole extraction, is expected.

Fig. 2 shows the results of TOF electron mobility measurements of $PC_{71}BM$. The electron transient is found to be rather dispersive as seen by the small angle between the plateau and tail in Fig. 2(a). With the MoO_3 electrode, no charging of the film was observed. The transit time reduces strongly with increasing electric field, indicating a positive electric field dependence of the mobility. At a field strength of 9×10^4 V/cm the mobility is 1×10^{-3} cm²/Vs with an error range of $\pm 2 \times 10^{-4}$ cm²/Vs obtained from two different samples and two different pixels each. Our measurements show that the hole and electron mobilities of PTB7 and $PC_{71}BM$ respectively are very similar, suggesting that these materials could provide nicely balanced electron and hole transport in the blend.

3.3. Hole mobility of PTB7:$PC_{71}BM$ and temperature dependence

In photovoltaic devices, blends of PTB7 with $PC_{71}BM$ are used and the blend morphology can additionally impact the mobility for electrons and holes. In Fig. 3(a) the hole photocurrent transient of PTB7:$PC_{71}BM$ is shown for varying temperature, revealing a clear transit kink. Electron transients however were found to be very dispersive and an electron mobility could not be obtained. For higher temperatures, in the hole transients a slight first kink arises, similar to that observed in P3HT:$PC_{61}BM$ blends and attributed to a high degree of phase separation [20]. The hole mobility, taken from the second kink and the film thickness of 7.35 ± 0.3 µm, had a negative field dependence. This is typical for such blends [20,23] and is attributed to high spatial disorder [24]. The average mobility at a field strength of 2.2×10^4 V/cm is about 2×10^{-4} cm²/Vs (see Fig. 3(b)). The hole mobility in the blend is hence a factor of five lower than that of neat PTB7 due to the enhanced disorder and agrees well with values reported by SCLC measurements, which are between 5.4×10^{-5} cm²/Vs and 3.2×10^{-4} cm²/Vs [25–27].

As we are interested in how the mobility influences the device performance, we varied the temperature for TOF mobility

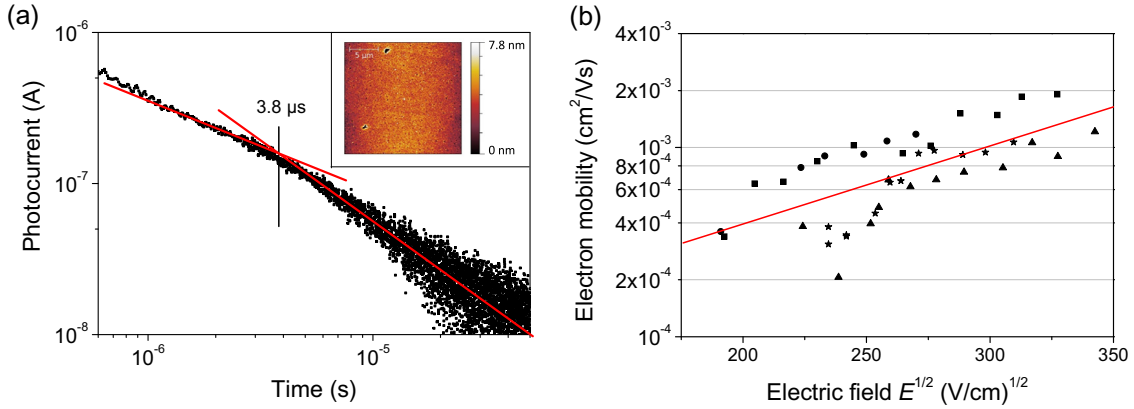

Fig. 2. (a) A typical electron photocurrent transient of $PC_{71}BM$ at an applied bias of 20 V and a film thickness of 2.8 µm. The inset shows an AFM image with 20 µm field of view, revealing low surface roughness. (b) The electron mobility of 2 different samples and 2 pixels each, as represented by different symbols. The red line shows a linear trend of the mobility, depending exponentially on the square root of the electric field. (For interpretation of the references to color in this figure legend, the reader is referred to the web version of this article.)

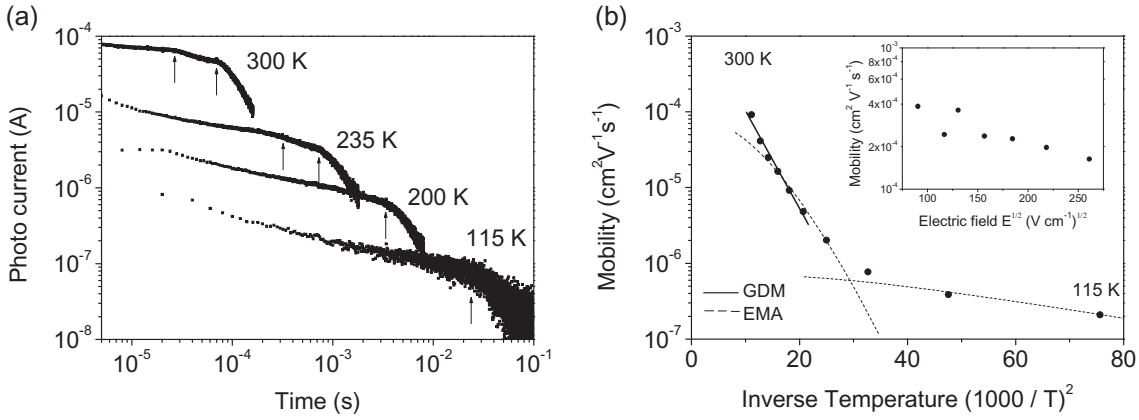

Fig. 3. (a) Temperature dependence of PTB7:$PC_{71}BM$ hole transients at an applied field of 9.5×10^4 V/cm and a film thickness of 7.35 μm. Arrows indicate kinks. (b) With reducing temperature the mobility drops by three orders of magnitude. At higher temperatures an exponential decrease is found for the mobility vs. $1/T^2$ according to the Gaussian disorder model (GDM) [28]. The dashed lines are fits of an effective medium approach (EMA) including traps [7]. The inset shows the electric field dependence at room temperature.

measurements of PTB7:$PC_{71}BM$ blends. The mobility is strongly dependent on temperature, increasing exponentially by three orders of magnitude from 115 K to 300 K, see Fig. 3(b).

From the temperature dependence of the mobility, the charge transport parameters of the Gaussian disorder model can be determined [28]. Plotting the hole mobility of PTB7:$PC_{71}BM$ blends against the inverse square of the temperature, T^{-2}, on a semilog scale gives a linear relationship in the high temperature regime, according to Eq. (4), with the slope related to the width of the density of states σ, the mobility at infinite temperature μ_0, the characteristic temperature T_0 and the Boltzmann constant k.

$$\mu = \mu_0 e^{-\left(\frac{T_0}{T}\right)^2} \quad (4.1), \qquad \sigma = \frac{3}{2} k T_0 \quad (4.2) \tag{4}$$

Hole transport of PTB7:$PC_{71}BM$ has a μ_0 of 2.0×10^{-3} cm^2/Vs and σ of 70 meV. The temperature dependence was also analyzed with an effective medium approach (EMA) including trap states according to Fishchuk et al. [7]. Although the condition of high energetic disorder ($\sigma/kT \gg 1$) is not clearly fulfilled, fits according to Eqs. (5.2) and (5.3) were applied. Where E_t is the trap energy, c is the concentration of trap states compared to conduction states, T_{Cr} is the critical temperature at which charge transport via trap states becomes dominant, σ_0 and σ_1 are the width of the Gaussian energy distribution of conduction and trap states respectively (taken as equal) and μ_0 is the trap-free mobility.

$$T_{Cr} = -\frac{E_t}{2k \ln(c)} \quad (5.1)$$

$$T > T_{Cr}: \quad \mu = \frac{\mu_0}{c} \frac{\sigma_0}{kT} \exp\left(-\frac{E_t}{2kT}\left(\frac{\sigma_1}{kT}\right)^2\right) \quad (5.2) \tag{5}$$

$$T < T_{Cr}: \quad \mu = \mu_0 c \frac{\sigma_0}{kT} \exp\left(-0.5\left(\frac{\sigma_1}{kT}\right)^2\right) \quad (5.3)$$

The fits are shown as dashed lines in Fig. 3(b) and show good agreement with the experimental data. Parameters of the trap energy of 0.1 eV and the trap concentration of 8% are obtained. The trap energy is hence comparable to the width of the density of states which implies that trapping originates from the tail states, as has been observed in P3HT [29].

3.4. Temperature dependence of PTB7:$PC_{71}BM$ devices

An interesting and yet not clearly understood question is how the charge carrier mobility relates to the photovoltaic operation of the device. As detailed in the introduction section, recombination and extraction dynamics strongly influence the solar cell performance and depend on the mobility. Drift–diffusion modeling has revealed optimum electron and hole mobilities of about 10^{-2}–10^{-3} cm^2/Vs with a relatively flat maximum [8–10]. The temperature dependence offers a simple and effective way to tune the mobility and allows its effect on solar cell characteristics to be observed.

At room temperature the PTB7:$PC_{71}BM$ devices had a power conversion efficiency of 6.9% (JV-curves are shown in Fig. 4). This fell to 2.5% when the solar cells were cooled to 77 K. The device parameters versus temperature and hole mobility are shown in Fig. 7. The loss is due to a reduced short circuit current density (J_{SC}) of 8.1 mA/cm^2 at 77 K compared to 12.9 mA/cm^2 at 295 K and the *FF* reduced to 33% compared to 65%. The open circuit voltage (V_{OC}) decreases linearly with temperature. Various models exist for the origin of the V_{OC} and could be applied to explain the increase with reducing temperature, such as a shift of the quasi Fermi-levels [30], reduced dark injection [31], reduced recombination [32] and an increased charge density in the active layer [11]. The concept of the quasi-Fermi level shift as a function of temperature leads to

$$V_{OC} = \frac{E_{gap}}{e} - \frac{kT}{e} \ln\left(\frac{N^2}{np}\right) \tag{6}$$

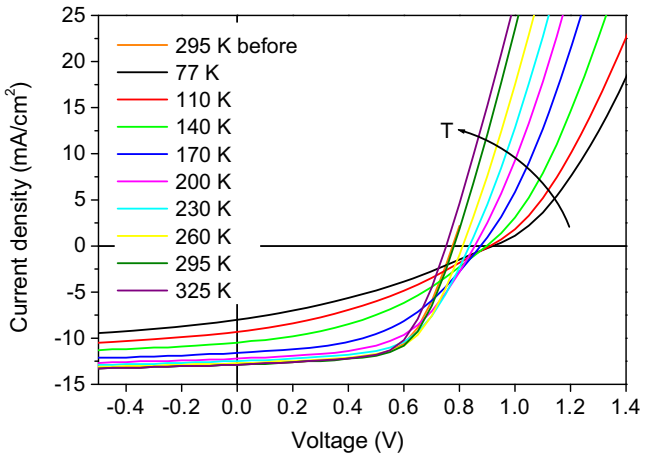

Fig. 4. Temperature dependence of the JV-characteristics of PTB7:$PC_{71}BM$ with an active layer thickness of 80 nm. The efficiency drops to about half of its room temperature value.

where N is the density of conduction states and E_{gap} is the effective band gap, and provided the best agreement with our experimental data. The charge carrier densities np increase by about a factor of two when the sample is cooled to 77 K (as shown in the SI) but have, due to the logarithm in Eq. (6), minor influence on the V_{OC} [33]. The V_{OC} is thus mainly influenced by the temperature [9]. Extrapolation of the V_{OC} to 0 K gives the effective band gap of the blend [34] which resulted in 1.0 eV, in good agreement with the value derived from the energy levels [35,1]. Rauh et al. found a deviation of the linear dependence of the V_{OC} for PTB7:$PC_{71}BM$ samples at low temperature and attributed this to inefficient charge extraction due to a contact barrier [36]. This could not be confirmed by the devices shown here. Upon warming up to room temperature the device performance fully recovered and the characteristics were identical to before the cooling cycle. If we consider that at a temperature of 77 K the hole mobility is reduced by factor of a thousand, it is remarkable that the solar cells still perform reasonably well.

Besides the mobility a few material parameters are influenced by the temperature. One is that the absorption spectrum and hence the EQE might change. In Fig. 5(a) the absorption spectrum of a PTB7:$PC_{71}BM$ blend is shown at room temperature and liquid nitrogen temperature. The spectrum shows only minor changes as in the region of 650 nm with a more pronounced valley between the peaks. The EQE, however decreases when the sample is cooled as shown in Fig. 5(b). The integrals of the EQE spectra resemble the trend of J_{SC} with a reduction of 35% when cooled to 77 K, but the shape of the spectra remained unchanged. Hence the number of absorbed photons remains constant when cooling to liquid nitrogen but the current decreases due to increased recombination.

In order to get further insight into the recombination kinetics we also varied the light intensity during the measurement of JV-characteristics and the results are shown in Fig. 6. The plot of J_{SC} versus intensity I on a log–log scale provides a good estimate of bimolecular recombination losses at 0 V [37,38]. The traces in Fig. 6(a) have been fitted with a power law, $J_{SC} = aI^b$, as a linear fit on logarithmic scales. The exponent b reduces with decreasing temperature from 0.968 to 0.917 denoting an increase of bimolecular recombination losses. This can be explained by a slower charge extraction at a reduced mobility and thereby a higher amount of charge carriers stored in the device. This results in the increase of bimolecular recombination as it depends on the square of the charge carrier density. At low temperature the FF is reduced because of the higher series resistance and increased bimolecular recombination. With reduced light intensity the charge density in the active layer reduces and the FF improves, as at 77 K it increases from 33% at 1 sun intensity to 66% at 0.01 sun (see Fig. S4).

From plots of the open circuit voltage against the natural logarithm of light intensity, the amount of monomolecular recombination can be judged [30,36]. If the slope equals kT/e, no trap assisted recombination appears. As shown in Fig. 6(b), the slopes of PTB7:$PC_{71}BM$ increase from 1.07 kT/e to 1.93 kT/e, when the temperature decreases from 300 K to 77 K, which corresponds to a drastic increase in SRH recombination. Stronger occupation of traps at low temperature is expected as charge carriers are no longer provided with thermal energy to escape from the tail states.

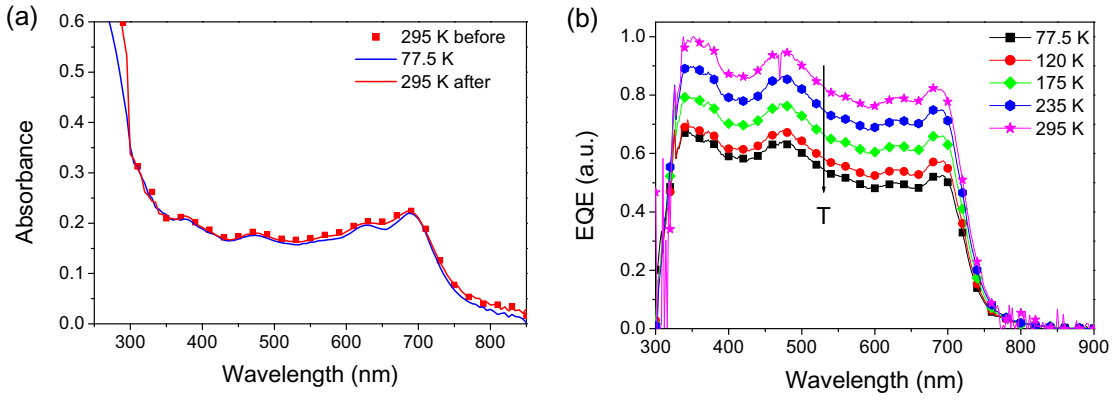

Fig. 5. (a) The absorption spectrum of PTB7:$PC_{71}BM$ at room temperature (red dots and line) before and after cooling to 77.4 K (blue line). (b) Temperature dependence of the EQE spectrum of PTB7:$PC_{71}BM$ normalized to maximum at 295 K. (For interpretation of the references to color in this figure legend, the reader is referred to the web version of this article.)

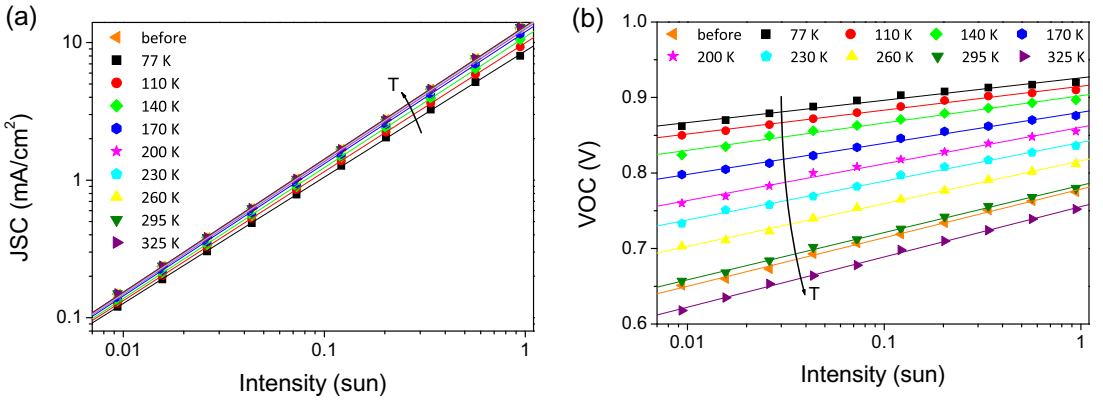

Fig. 6. Device parameters of PTB7:$PC_{71}BM$ as a function of intensity and temperature. (a) J_{SC} vs. light intensity on log–log plots. (b) V_{OC} vs. light intensity on semi-log scale. Straight lines are linear fits.

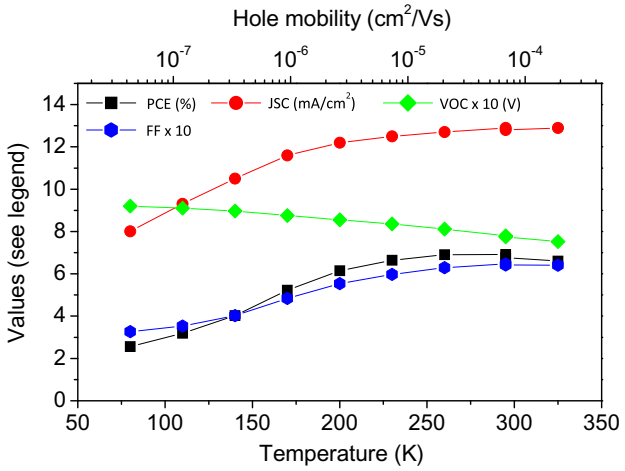

Fig. 7. Device parameters vs. temperature and mobility. The power conversion efficiency (PCE) of PTB7:$PC_{71}BM$ reaches a maximum performance at room temperature due to a trade-off between J_{SC}, FF and V_{OC}.

As shown in Fig. 7 the device parameters vs. temperature give a clear maximum for the power conversion efficiency of PTB7:$PC_{71}BM$ solar cells between 260 K and 295 K. At higher temperature (325 K) the J_{SC} and FF have flattened but as the V_{OC} decreases linearly, the efficiency begins to drop. The parameters of J_{SC} and FF are directly influenced by the mobility, whereas the V_{OC} is additionally influenced by the temperature due to a shift of the quasi-Fermi levels. For temperature increases above room temperature, the effects of increased mobility on J_{SC} and FF are outweighed by the decrease of V_{OC}. For the system studied of PTB7:$PC_{71}BM$, with a film thickness of 80 nm, the efficiency decreases from 6.9% at room temperature by only 0.3% when the hole mobility is reduced (by lowering the temperature) by an order of magnitude from 7×10^{-5} cm^2/Vs to 7×10^{-6} cm^2/Vs. This shows the rather weak influence of the mobility near the optimum and is qualitatively in agreement with theory [8–11].

4. Conclusion

In conclusion, we investigated the charge carrier mobility of the important solar materials PTB7, $PC_{71}BM$ and the blend PTB7:$PC_{71}BM$ by the time of flight technique. High hole mobility of about 1×10^{-3} cm^2/Vs was observed in neat PTB7 and the same value was observed for the electron mobility of $PC_{71}BM$. The hole mobility of PTB7 is almost an order of magnitude higher than that of P3HT and well balanced with the electron mobility of $PC_{71}BM$, providing a reason for the higher EQE and fill factors generally observed. The temperature dependence of PTB7:$PC_{71}BM$ revealed a fast drop of the hole mobility in PTB7:$PC_{71}BM$ by three orders of magnitude when cooled from room temperature to 77 K. With reducing the mobility in PTB7:$PC_{71}BM$ solar cells we found that bimolecular and Shockley–Read–Hall recombination increased, because of the longer sweep-out time and thereby higher charge density in the active layer. SRH recombination was identified as the dominant recombination mechanism at low temperature. The optimum of the device performance occurred at room temperature. Our results suggest that tuning the mobility by variation of the temperature is an effective way to determine the losses and the potential for optimization of a materials system.

Acknowledgements

This research was financially supported by the EPSRC of the UK, grant EP/I00243X. IDWS is A Royal Society Wolfson Research Merit Award holder. The funding agencies had no influence on the preparation of the manuscript and on the decision to which journal it is submitted.

Appendix A. Supplementary data

Supplementary data associated with this article can be found, in the online version, at http://dx.doi.org/10.1016/j.orgel.2015.03.013.

References

[1] Z. He, C. Zhong, S. Su, M. Xu, H. Wu, Y. Cao, Enhanced power-conversion efficiency in polymer solar cells using an inverted device structure, Nat. Photon. 6 (2012) 593–597, http://dx.doi.org/10.1038/nphoton.2012.190.
[2] A. Pivrikas, G. Juška, A. Mozer, M. Scharber, K. Arlauskas, N. Sariciftci, et al., Bimolecular recombination coefficient as a sensitive testing parameter for low-mobility solar-cell materials, Phys. Rev. Lett. 94 (2005) 176806, http://dx.doi.org/10.1103/PhysRevLett.94.176806.
[3] L.J.A. Koster, V.D. Mihailetchi, P.W.M. Blom, Bimolecular recombination in polymer/fullerene bulk heterojunction solar cells, Appl. Phys. Lett. 88 (2006) 052104, http://dx.doi.org/10.1063/1.2170424.
[4] W. Shockley, W.T. Read Jr, Statistics of the recombinations of holes and electrons, Phys. Rev. 87 (1952) 835.
[5] R.N. Hall, Electron-hole recombination in germanium, Phys. Rev. 87 (1952) 387.
[6] S.R. Cowan, W.L. Leong, N. Banerji, G. Dennler, A.J. Heeger, Identifying a threshold impurity level for organic solar cells: enhanced first-order recombination via well-defined PC84BM traps in organic bulk heterojunction solar cells, Adv. Funct. Mater. 21 (2011) 3083–3092, http://dx.doi.org/10.1002/adfm.201100514.
[7] I.I. Fishchuk, A.K. Kadashchuk, H. Bässler, D.S. Weiss, Nondispersive charge-carrier transport in disordered organic materials containing traps, Phys. Rev. B 66 (2002) 205208.
[8] C. Deibel, A. Wagenpfahl, V. Dyakonov, Influence of charge carrier mobility on the performance of organic solar cells, Phys. Stat. Sol. 2 (2008) 175–177, http://dx.doi.org/10.1002/pssr.200802110.
[9] W. Tress, K. Leo, M. Riede, Optimum mobility, contact properties, and open-circuit voltage of organic solar cells: a drift-diffusion simulation study, Phys. Rev. B 85 (2012) 155201, http://dx.doi.org/10.1103/PhysRevB.85.155201.
[10] O. Ramírez, V. Cabrera, L.M. Reséndiz, Optimum ratio of electron-to-hole mobility in P3HT:PCBM organic solar cells, Opt. Quant. Electron. (2013) 1291–1296, http://dx.doi.org/10.1007/s11082-013-9855-1.
[11] M.M. Mandoc, L.J.A. Koster, P.W.M. Blom, Optimum charge carrier mobility in organic solar cells, Appl. Phys. Lett. 90 (2007) 133504, http://dx.doi.org/10.1063/1.2711534.
[12] C.M. Proctor, J.A. Love, T.-Q. Nguyen, Mobility guidelines for high fill factor solution-processed small molecule solar cells, Adv. Mater. 26 (2014) 5957–5961, http://dx.doi.org/10.1002/adma.201401725.
[13] B. Philippa, M. Stolterfoht, P.L. Burn, G. Juška, P. Meredith, R.D. White, et al., The impact of hot charge carrier mobility on photocurrent losses in polymer-based solar cells (2014). Preprint arXiv:1403.0311.
[14] H. Scher, E.W. Montroll, Anomalous transit-time dispersion in amorphous solids, Phys. Rev. B. 12 (1975) 2455–2477, http://dx.doi.org/10.1103/PhysRevB.12.2455.
[15] J. Simmons, Poole–Frenkel effect and Schottky effect in metal–insulator–metal systems, Phys. Rev. 155 (1967) 657–660, http://dx.doi.org/10.1103/PhysRev.155.657.
[16] S. Foster, F. Deledalle, A. Mitani, T. Kimura, K.-B. Kim, T. Okachi, et al., Electron collection as a limit to polymer:PCBM solar cell efficiency: effect of blend microstructure on carrier mobility and device performance in PTB7:PCBM, Adv. Energy Mater. (2014) 1400311, http://dx.doi.org/10.1002/aenm.201400311.
[17] Y. Liang, Z. Xu, J. Xia, S.-T. Tsai, Y. Wu, G. Li, et al., For the bright future–bulk heterojunction polymer solar cells with power conversion efficiency of 7.4%, Adv. Mater. 22 (2010) E135–E138, http://dx.doi.org/10.1002/adma.200903528.
[18] N. Zhou, H. Lin, S.J. Lou, X. Yu, P. Guo, E.F. Manley, et al., Morphology–performance relationships in high-efficiency all-polymer solar cells, Adv. Energy Mater. 4 (2014) 1300785, http://dx.doi.org/10.1002/aenm.201300785.
[19] R.L. Uy, S.C. Price, W. You, Structure–property optimizations in donor polymers via electronics, substituents, and side chains toward high efficiency solar cells, Macromol. Rapid Commun. 33 (2012) 1162–1177, http://dx.doi.org/10.1002/marc.201200129.
[20] A. Baumann, J. Lorrmann, C. Deibel, V. Dyakonov, Bipolar charge transport in poly(3-hexyl thiophene)/methanofullerene blends: a ratio dependent study, Appl. Phys. Lett. 93 (2008) 252104, http://dx.doi.org/10.1063/1.3055608.
[21] S.M. Tuladhar, D. Poplavskyy, S.A. Choulis, J.R. Durrant, D.D.C. Bradley, J. Nelson, Ambipolar charge transport in films of methanofullerene and poly(phenylenevinylene)/methanofullerene blends, Adv. Funct. Mater. 15 (2005) 1171–1182, http://dx.doi.org/10.1002/adfm.200400337.

[22] M. Kröger, S. Hamwi, J. Meyer, T. Riedl, W. Kowalsky, A. Kahn, P-type doping of organic wide band gap materials by transition metal oxides: a case-study on molybdenum trioxide, Org. Electron. 10 (2009) 932–938, http://dx.doi.org/10.1016/j.orgel.2009.05.007.
[23] A.M. Ballantyne, L. Chen, J. Dane, T. Hammant, F.M. Braun, M. Heeney, et al., The effect of poly(3-hexylthiophene) molecular weight on charge transport and the performance of polymer: fullerene solar cells, Adv. Funct. Mater. 18 (2008) 2373–2380, http://dx.doi.org/10.1002/adfm.200800145.
[24] A.J. Mozer, N.S. Sariciftci, Negative electric field dependence of charge carrier drift mobility in conjugated, semiconducting polymers, Chem. Phys. Lett. 389 (2004) 438–442, http://dx.doi.org/10.1016/j.cplett.2004.04.001.
[25] G.D.M.R. Dabera, K.D.G.I. Jayawardena, M.R.R. Prabhath, I. Yahya, Y.Y. Tan, N.A. Nismy, et al., Hybrid carbon nanotube networks as efficient hole extraction layers for organic photovoltaics, ACS Nano 7 (2013) 556–565, http://dx.doi.org/10.1021/nn304705t.
[26] H. Zhou, Y. Zhang, J. Seifter, S.D. Collins, C. Luo, G.C. Bazan, et al., High-efficiency polymer solar cells enhanced by solvent treatment, Adv. Mater. 25 (2013) 1646–1652, http://dx.doi.org/10.1002/adma.201204306.
[27] Z. He, C. Zhong, X. Huang, W.-Y. Wong, H. Wu, L. Chen, et al., Simultaneous enhancement of open-circuit voltage, short-circuit current density, and fill factor in polymer solar cells, Adv. Mater. 23 (2011) 4636–4643, http://dx.doi.org/10.1002/adma.201103006.
[28] H. Bässler, Charge transport in disordered organic photoconductors a Monte Carlo simulation study, Phys. Stat. Sol. 175 (1993) 15–56.
[29] J. Schafferhans, A. Baumann, C. Deibel, V. Dyakonov, Trap distribution and the impact of oxygen-induced traps on the charge transport in poly(3-hexylthiophene), Appl. Phys. Lett. 93 (2008) 093303, http://dx.doi.org/10.1063/1.2978237.
[30] L.J.A. Koster, V.D. Mihailetchi, R. Ramaker, P.W.M. Blom, Light intensity dependence of open-circuit voltage of polymer:fullerene solar cells, Appl. Phys. Lett. 86 (2005) 123509, http://dx.doi.org/10.1063/1.1889240.
[31] R. Mauer, I.A. Howard, F. Laquai, Effect of nongeminate recombination on fill factor in polythiophene/methanofullerene organic solar cells, J. Phys. Chem. Lett. 1 (2010) 3500–3505, http://dx.doi.org/10.1021/jz101458y.
[32] D. Credgington, J.R. Durrant, Insights from transient optoelectronic analyses on the open-circuit voltage of organic solar cells, J. Phys. Chem. Lett. 3 (2012) 1465–1478, http://dx.doi.org/10.1021/jz300293q.
[33] D. Rauh, A. Wagenpfahl, C. Deibel, V. Dyakonov, Relation of open circuit voltage to charge carrier density in organic bulk heterojunction solar cells, Appl. Phys. Lett. 98 (2011) 133301, http://dx.doi.org/10.1063/1.3566979.
[34] S.R. Cowan, A. Roy, A.J. Heeger, Recombination in polymer–fullerene bulk heterojunction solar cells, Phys. Rev. B 82 (2010) 245207, http://dx.doi.org/10.1103/PhysRevB.82.245207.
[35] C.J. Brabec, A. Cravino, D. Meissner, N.S. Sariciftci, T. Fromherz, M.T. Rispens, et al., Origin of the open circuit voltage of plastic solar cells, Adv. Funct. Mater. 11 (2001) 374–380.
[36] D. Rauh, C. Deibel, V. Dyakonov, Charge density dependent nongeminate recombination in organic bulk heterojunction solar cells, Adv. Funct. Mater. 22 (2012) 3371–3377, http://dx.doi.org/10.1002/adfm.201103118.
[37] A.K.K. Kyaw, D.H. Wang, V. Gupta, W.L. Leong, L. Ke, G.C. Bazan, et al., Intensity dependence of current-voltage characteristics and recombination in high-efficiency solution-processed small-molecule solar cells, ACS Nano 7 (2013) 4569–4577, http://dx.doi.org/10.1021/nn401267s.
[38] I. Riedel, J. Parisi, V. Dyakonov, L. Lutsen, D. Vanderzande, J.C. Hummelen, Effect of temperature and illumination on the electrical characteristics of polymer–fullerene bulk-heterojunction solar cells, Adv. Funct. Mater. 14 (2004) 38–44, http://dx.doi.org/10.1002/adfm.200304399.